



Contents lists available at ScienceDirect

The Journal of Foot & Ankle Surgery

journal homepage: www.jfas.org

Original Research

Weightbearing CT-based predictive surgical planning for joint-sparing reconstruction of progressive collapsing foot deformity

Wolfram Grün, MD^{a,b,c}, Pierre-Henri Vermorel, MD^{a,d,e}, Antoine Acker, MD^{a,f}, Emily J. Luo, MHSc^a, Enrico Pozzessere, MD^a, Scott J. Ellis, MD^g, Francois Lintz, MD, PhD^{a,h}, Cesar de Cesar Netto, MD, PhD^{a,*}

^a Department of Orthopaedic Surgery, Duke University School of Medicine, Durham, NC, USA

^b Division of Orthopaedic Surgery, Oslo University Hospital, Oslo, Norway

^c Department of Orthopaedic Surgery, Østfold Hospital Trust, Grålum, Norway

^d Inter-university Laboratory of Human Movement Science, University Lyon - University Jean-Monnet Saint-Étienne, Saint-Etienne, France

^e Department of Orthopaedic Surgery, University Hospital Centre of Saint-Étienne, Saint-Étienne, France

^f Centre of Foot and Ankle Surgery, Clinique La Colline, Geneva, Switzerland

^g Hospital for Special Surgery, New York, NY, USA

^h Ramsay Healthcare Clinique de l'Union, Saint-Jean, Toulouse, France

ARTICLE INFO

Level of Clinical Evidence: 4
retrospective case series

Keywords:

Flatfoot
Joint-sparing reconstruction
Predictive modeling
Patient-specific planning
Medial displacement calcaneal osteotomy
Lateral column lengthening
Cotton osteotomy
Hindfoot alignment

ABSTRACT

Background: Progressive Collapsing Foot Deformity (PCFD) is a complex multiplanar deformity commonly treated with osteotomy-based reconstruction in flexible cases. Although weightbearing CT (WBCT) has improved assessment of PCFD, WBCT-based predictive planning models remain unexplored.

Purpose: To evaluate the accuracy of a WBCT-based predictive surgical planning model in estimating postoperative alignment following reconstruction for flexible PCFD.

Study design: Retrospective cohort study

Methods: Thirty-four patients with PCFD who underwent reconstruction with medial displacement calcaneal osteotomy, lateral column lengthening, and/or first-ray plantarflexion osteotomy and had preoperative and 3-month postoperative WBCT were included. The model estimated postoperative hindfoot moment arm (HMA), axial talus–first metatarsal angle (TFMA-A), talonavicular coverage angle (TNCA), and sagittal talus–first metatarsal angle (TFMA-S) using correction magnitudes. Predicted alignment was compared with postoperative WBCT measurements using Bland–Altman analysis, mean absolute error (MAE), root-mean-square error (RMSE), and paired t-tests.

Results: Predictive accuracy was highest for HMA, with a mean bias of +2.73 mm ($p = 0.005$), narrowest limits of agreement (–7.66 mm to +13.12 mm), and lowest MAE and RMSE values (approximately 2.9 mm and 3.7 mm). TFMA-A, TNCA, and TFMA-S demonstrated wider limits of agreement (approximately –17° to +21°) and greater case-level variability, although no significant systematic differences between predicted and postoperative values were observed ($p = 0.21–0.90$).

Conclusions: A WBCT-based predictive surgical planning model estimated postoperative alignment accurately for hindfoot valgus correction, while predictions of midfoot/forefoot abduction and arch collapse demonstrated greater individual variability. Despite this variability, the model accurately reproduced mean multiplanar correction, supporting patient-specific surgical planning in PCFD.

© 2026 by the American College of Foot and Ankle Surgeons. All rights are reserved, including those for text and data mining, AI training, and similar technologies.

Institution at which the work was performed: Duke Healthcare Orthopedics at Arrington, Foot and Ankle Division

*Corresponding author at: Cesar de Cesar Netto, Department of Orthopaedic Surgery, Duke University, 5601 Arrington Park Drive, Suite 300, Morrisville, NC 27560, USA.

E-mail address: cesar.netto@duke.edu (C. de Cesar Netto).

Introduction

Progressive Collapsing Foot Deformity (PCFD) is a complex, multiplanar condition typically involving hindfoot valgus (Class A), midfoot/forefoot abduction (Class B), collapse of the medial arch (Class C), as well as peritalar subluxation (Class D) and possible valgus talar tilt (Class E) [1,2] These deformity classes may present in isolation or in

combination and are stratified by flexibility. Flexible deformities (stage 1) are typically amenable to joint-sparing reconstruction, whereas rigid deformities (stage 2) often require hindfoot arthrodeses.

Operative management of flexible PCFD is recommended when nonoperative measures have failed and usually involves a combination of joint-sparing realignment techniques such as Medial Displacement Calcaneal Osteotomy (MDCO) to address Class A deformity, Lateral Column Lengthening (LCL) to target Class B abduction deformity, and Cotton osteotomy (CO) to restore Class C deformity, in addition to various soft tissue procedures [3–7]. Achieving optimal correction remains challenging due to heterogeneous deformity patterns and experience-based surgical planning [8–10].

Previous efforts have primarily relied on conventional weightbearing radiographs to evaluate the individual corrective effects of MDCO, LCL and CO [11–13]. However, these studies assessed each procedure in isolation and did not explore their combined impact on multiplanar deformity correction in PCFD.

Recent advances in weightbearing computed tomography (WBCT) have substantially improved the understanding of the three-dimensional pathoanatomy of PCFD [14,15]. WBCT studies have underscored that peritalar subluxation (PTS) plays a central role in both the onset and progression of the deformity, highlighting the need for 3D-based assessment and surgical planning [16,17]. However, WBCT-based predictive models specifically designed to estimate achieved surgical correction following PCFD reconstruction remain unexplored. The development of a WBCT-based predictive surgical planning model for PCFD – particularly with respect to the three most commonly performed bony procedures (MDCO, LCL, and CO) – has the potential to meaningfully advance surgical management of PCFD.

In this study, our objective was to evaluate the effectiveness of a WBCT-based predictive surgical planning model for patients with flexible PCFD undergoing joint-sparing reconstruction. We compared model-predicted alignment with actual postoperative results. We hypothesized that the WBCT-based predictive surgical planning model would accurately predict postoperative alignment, closely matching clinical outcomes.

Patients And Methods

This institutional review board (IRB)-approved retrospective study (IRB number Pro00113556) included a consecutive series of adult patients who underwent joint-sparing surgical correction of flexible PCFD by a single surgeon at a single institution and who had both preoperative and three-months postoperative WBCT scans obtained as part of routine clinical practice. The operating surgeon was a board-certified, fellowship-trained foot and ankle surgeon with 15 years of experience who performed approximately 60 PCFD reconstructions annually. Postoperative WBCT scans were obtained after three months, reflecting standard clinical practice for assessment of initially achieved correction under full weightbearing following bony healing. Patients with Class E ankle valgus deformity were excluded as talar tilt may influence associated foot alignment parameters [18]. In all cases, the treating surgeon independently selected the type and magnitude of corrective procedures based on preoperative WBCT findings, clinical examination, and intraoperative assessment of residual alignment and correction goals. Hindfoot valgus severity, midfoot/forefoot abduction, medial arch collapse, and the presence of residual forefoot varus or instability were considered when determining the need for MDCO, LCL, and first-ray plantarizing procedures, as well as the magnitude of correction applied.

WBCT scans (CurveBeamAI®, Hatfield, PA) were obtained between December 2022 and May 2024 using a standardized clinical acquisition protocol. Patients with previous PCFD surgery or who were enrolled in an ongoing prospective study (IRB number Pro114640) were excluded.

Baseline demographics, timing of preoperative and postoperative WBCT scans, and procedural details were recorded, including whether MDCO, LCL, or first-ray plantarizing procedures (CO or Lopicotton [19,20]) were performed and the magnitude of correction applied (i.e. how many millimeters of medial translation for MDCO and the wedge size in mm for LCL, CO and Lopicotton). Soft-tissue procedures were documented.

Semi-automated measurements

Semi-automated measurements of pre- and postoperative WBCT images were obtained using BoneLogic® software (Disior®; Paragon 28®/Zimmer Biomet®, Warsaw, IN), to assess PCFD Class A, B and C (Fig. 1). Hindfoot valgus (PCFD Class A) was quantified using the hindfoot moment arm (HMA), defined as the mediolateral distance (mm) between the tibial axis and the most inferior point of the calcaneus, with positive values indicating valgus alignment. The axial talus–first metatarsal angle (TFMA-A), defined as the angle between the longitudinal axes of the talus and the first metatarsal in the axial plane, and the talonavicular coverage angle (TNCA), defined as the angle between the longitudinal axes of the talus and navicular, were used to quantify forefoot abduction (PCFD Class B), with positive values indicating forefoot abduction. Collapse of the medial column (PCFD Class C) was assessed using the sagittal talus–first metatarsal angle (TFMA-S), defined as the angle between the longitudinal axes of the talus and first metatarsal in the sagittal plane, where negative values indicated medial arch collapse commonly seen in

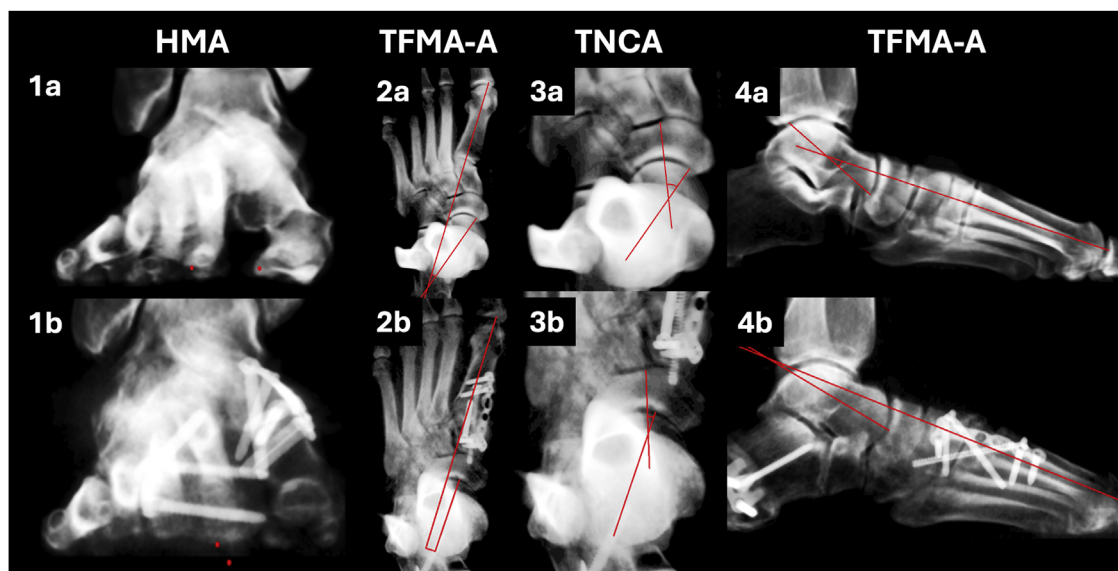


Fig. 1. Preoperative (row 1) and postoperative (row 2) WBCT-derived semi-automated measurements generated using Disior/BoneLogic segmentation for a representative patient treated with medial displacement calcaneal osteotomy (MDCO, 11 mm), lateral column lengthening (6 mm), and Lopicotton first-TMT plantarflexion arthrodesis using a 10 mm allograft wedge. Four alignment parameters are shown: hindfoot moment arm (HMA), talus–first metatarsal angle in the axial plane (TFMA-A), talonavicular coverage angle (TNCA), and talus–first metatarsal angle in the sagittal plane (TFMA-S). Preoperative values were: HMA 21.64 mm (1a), TFMA-A 18.39° (1b), TNCA 41.35° (1c), and TFMA-S – 22.94° (1d). Postoperative values were: HMA 3.36 mm (2a), TFMA-A 1.79° (2b), TNCA 20.81° (2c), and TFMA-S – 8.79° (2d).

PCFD. Class D measurements were not included, as these parameters are not currently incorporated into the surgical planning model.

Surgical planning model

A WBCT-based predictive surgical planning model was used to estimate postoperative alignment following PCFD correction. This study represents the first description and clinical application of the predictive model. The model was developed using retrospective clinical WBCT datasets combined with cadaveric simulations of isolated and combined corrective procedures, including medial displacement calcaneal osteotomy (MDCO), lateral column lengthening (LCL), and Cotton osteotomy (CO). The algorithm is based on multivariable regression modeling linking preoperative WBCT alignment parameters and osteotomy magnitudes to predicted postoperative alignment changes for PCFD Classes A, B, and C. Variables incorporated into the model included preoperative deformity measurements, procedure type, and osteotomy magnitude for each corrective procedure. The model estimates postoperative correction using statistical relationships from the development dataset. Although the algorithm was developed using Cotton osteotomies, Lapidus procedures performed in the present study were treated as functionally equivalent first-ray plantarizing corrections based on wedge magnitude. Soft-tissue procedures were not incorporated into the model; therefore, the model estimates alignment changes attributable to bony correction alone. The model was used solely to generate predicted postoperative alignment based on the actual intraoperative correction magnitudes performed in each patient.

Testing scenario

Based on the preoperative WBCT scans, the predictive model generated predicted postoperative values for HMA (Class A), TFMA-A and TNCA (Class B) and TFMA-S (Class C) using the intraoperative magnitudes of MDCO, LCL, and first-ray procedures. Differences between preoperative and predicted postoperative values ($\Delta_{\text{Predicted}}$) and between the preoperative and true postoperative values (Δ_{Real}) were calculated for all parameters.

Statistics

Statistical analysis included computation of mean bias ($\Delta_{\text{Predicted}}$ minus Δ_{Real}), standard deviation (SD), and 95% limits of agreement (LoA) using Bland–Altman analysis [21]. LoA were prioritized over confidence intervals of the mean bias to characterize case-level prediction error. Paired t-tests were used to detect systematic differences between predicted and actual postoperative outcomes. Mean absolute error (MAE) and root-mean-square error (RMSE) were calculated to quantify prediction accuracy. The direction and magnitude of the bias (Predicted – Real) were used to characterize systematic tendencies of over- or underestimation, where positive bias indicated overestimation of correction and negative bias indicated underestimation. The qualitative interpretation of overall algorithm performance combined the direction of bias, and the width of the 95% LoA. Statistical significance was set at $p < 0.05$. All analyses were performed using Stata® 18.0 (StataCorp LLC®, College Station, TX).

Results

A total of 34 patients (19 females, 15 males) with a mean age of 51 ± 17.8 years and a mean body mass index of 31.7 ± 7.3 were included. The cohort included 21 right feet and 13 left feet. Preoperative WBCT scans were obtained a mean of 117.3 ± 89.1 days before surgery, while the follow-up WBCT scans were performed at a mean 89.7 ± 8.8 days after surgery.

MDCO was performed in 30 patients (88%), while LCL was added in 4 patients (12%). All patients (100%) underwent a first ray plantarizing procedure, consisting of either a CO in 19 cases (56%) or a Lapidus procedure in 15 cases (44%). No plantarizing TMT 1 fusions without a bone block (Lapidus) were performed (Table 1). Among soft-tissue procedures, Gastrocnemius recession or Achilles tendon lengthening was performed in 88% of patients, peroneal tendon procedures in 82%, posterior tibial tendon (PTT) related procedures including flexor digitorum longus (FDL) transfer in 76%, spring ligament reconstruction/augmentation in 59%, and superficial deltoid ligament reconstruction/augmentation in 53%.

Patient-level measurement data are summarized in Table 2, with preoperative, postoperative, and model-predicted values shown in Table 3 and Fig. 2.

Table 1

Magnitude of correction for medial displacement calcaneal osteotomy (MDCO), lateral column lengthening (LCL), and first-ray plantarizing procedures (Cotton or Lapidus) performed in the current study ($N = 34$).

Procedure	n	Median (range), mm	Mode, mm
MDCO	30	9.5 (6-14)	10
LCL	4	6 (6-6)	6
First ray procedure	34	8 (6-12)	10

Values are reported as median (range) and mode, calculated only in patients in whom the respective procedure was performed ($n =$ procedure-specific subgroup).

Model prediction accuracy

In the tested scenario, the model demonstrated the highest overall predictive accuracy for HMA, showing a small but statistically significant mean bias ($+2.73$ mm, $p = 0.005$) and the narrowest limits of agreement (-7.66 to $+13.12$ mm) (Table 3). Mean absolute error and RMSE were lowest for HMA (≈ 2.9 mm and ≈ 3.7 mm), indicating more consistent prediction of hindfoot realignment compared with the angular parameters. For TFMA-A, TNCA, and TFMA-S, prediction errors were larger and more variable, with wide limits of agreement (approximately -17 to 21°) and no significant systematic differences between predicted and actual postoperative values ($p = 0.21$ – 0.90) (Table 4). Despite close agreement in mean correction for Class B parameters, case-level variability remained high, resulting in broader limits of agreement and larger MAE and RMSE values (approximately 4 – 6°) (Table 4).

Discussion

This study evaluated the performance of a WBCT-based predictive surgical planning model designed to predict correction following PCFD reconstruction. Predictive accuracy was highest for Class A PCFD hindfoot valgus correction (HMA), whereas predictions of Class B (forefoot/midfoot abduction) and Class C (arch collapse) PCFD alignment (TNCA, TFMA-A and TFMA-S) demonstrated greater variability at the individual case level despite accurately matching the average magnitude of correction.

These findings align with prior work demonstrating predictable relationships between osteotomy magnitude and alignment change. MDCO has been shown to be the principal determinant of hindfoot realignment, with postoperative hindfoot alignment correlating with clinical outcomes [8,11]. Consistent with these observations, the predictive model reproduced postoperative hindfoot alignment with the narrowest limits of agreement. Midfoot/forefoot abduction (Class B) and medial arch restoration (Class C) are commonly addressed through lateral column lengthening and medial cuneiform osteotomies, respectively [5,12,13]. In this cohort, LCL was infrequently performed, suggesting that combined bony procedures contributed to abduction correction. While mean correction for TNCA, TFMA-A, and TFMA-S was accurately estimated, greater case-level variability was observed, likely reflecting unmodeled biological factors.

The interdependence of multiplanar deformity correction observed in this study is consistent with previously described coupling behavior, whereby calcaneal lengthening induces simultaneous changes in hindfoot, midfoot, and forefoot alignment [22]. Smith et al. further noted that combined procedures may generate greater multiplanar correction but increase the risk of lateral column overload [23]. The variability in our angular alignment predictions underscores the need for further refinement of predictive planning models to incorporate multiplanar coupling and soft-tissue effects.

Although soft-tissue procedures such as FDL transfer, spring and deltoid ligament augmentation are integral to PCFD correction, their isolated

Table 2
Patient-level data for the current study ($N = 34$), including preoperative Hindfoot Moment Arm (HMA), talus–first metatarsal angle in the axial plane (TFMA-A), talonavicular coverage angle (TNCA), and talus–first metatarsal angle in the sagittal plane (TFMA-S); the magnitude of bony procedures performed (mm); and the corresponding real postoperative and predicted postoperative values for HMA, TFMA-A, TNCA, and TFMA-S. HMA is reported in millimeters, whereas TFMA-A, TNCA, and TFMA-S are reported in degrees.

Patient number	Sex	Age	Preoperative measurements				Performed bony procedures			Real postoperative measurements				Predicted postoperative measurements			
			HMA	TFMA-A	TNCA	TFMA-S	MDCO	LCL	First ray procedure	HMA	TFMA-A	TNCA	TFMA-S	HMA	TFMA-A	TNCA	TFMA-S
1	F	48	11.4	25.2	42.1	-31.0	8	0	8	-3.4	14.9	33.2	-19.8	5.9	18.4	36.0	-18.8
2	F	55	11.3	25.2	43.7	-25.3	10	0	7	3.0	21.9	42.9	-22.7	3.1	14.7	33.9	-12.6
3	M	39	9.8	7.6	31.4	-13.9	6	0	6	3.7	12.5	34.2	-14.1	2.8	1.3	25.5	-5.7
4	F	46	5.2	30.4	45.4	-17.5	6	0	6	-1.1	4.3	21.6	-4.0	1.8	19.9	35.8	-13.7
5	F	72	13.4	32.9	53.1	-31.6	7	0	6	9.4	30.7	49.8	-29.1	8.6	25.4	45.8	-22.2
6	F	76	14.0	32.5	43.5	-32.4	10	0	10	18.1	31.7	43.0	-29.3	6.9	22.5	36.6	-18.0
7	M	38	13.9	14.9	33.6	-16.9	7	0	6	10.5	11.2	33.2	-13.1	5.9	7.8	27.9	-8.0
8	F	62	21.2	25.6	46.0	-31.2	9	0	7	8.3	27.5	48.6	-33.2	12.0	20.1	39.0	-15.5
9	F	65	2.0	17.9	40.4	-32.7	11	6	10	0.1	13.4	34.7	-28.2	-1.6	5.3	28.4	-11.5
10	F	59	13.4	22.9	41.1	-18.8	11	0	10	-7.7	-10.3	9.6	2.7	1.8	8.9	29.6	-6.6
11	M	45	17.1	22.9	49.2	-29.5	8	0	10	10.8	25.7	41.4	-14.6	10.8	18.1	41.7	-15.7
12	F	53	4.1	23.7	48.9	-11.9	6	0	8	-11.7	6.9	25.1	1.9	-1.1	10.9	34.0	-7.2
13	M	60	22.1	21.8	42.1	-37.3	13	0	12	10.9	19.4	34.7	-18.3	10.9	20.6	35.2	-8.7
14	M	71	17.5	41.9	55.1	-35.7	12	0	10	-4.3	29.2	44.6	-14.9	7.9	28.3	43.5	-19.6
15	M	17	20.0	30.7	48.5	-26.0	11	6	8	0.0	5.3	22.5	-8.7	4.9	13.3	32.6	-9.2
16	M	65	19.0	19.9	38.5	-44.1	14	0	12	7.3	21.7	37.5	-30.5	9.8	22.7	32.6	-8.3
17	M	39	14.2	27.1	44.8	-28.7	9	0	7	7.5	30.4	43.7	-27.4	6.8	18.7	36.9	-15.9
18	M	69	25.3	30.2	46.0	-27.2	14	0	12	-0.9	8.2	23.2	4.6	8.8	18.3	35.7	-7.5
19	F	37	23.8	23.3	47.0	-31.8	11	6	10	2.1	3.2	23.1	-7.5	7.8	13.1	31.5	-8.1
20	M	27	10.7	18.0	38.6	-21.2	10	0	8	-8.2	-0.3	23.2	-6.4	1.3	7.9	29.0	-7.9
21	M	72	11.3	30.2	43.1	-13.4	0	0	10	7.0	29.2	42.2	-7.6	9.0	20.7	35.6	-10.5
22	F	67	1.8	20.7	37.6	-25.1	0	0	12	-3.8	17.5	29.4	-9.9	6.9	21.1	43.0	-25.1
23	F	57	10.3	25.9	40.8	-15.3	9	0	7	6.1	21.6	35.0	-8.1	1.9	12.6	30.1	-8.4
24	F	67	9.9	27.5	41.5	-33.8	10	0	6	2.4	20.5	37.1	-19.2	3.1	18.5	33.2	-18.1
25	F	26	17.2	23.5	44.9	-22.4	8	0	10	1.9	20.1	35.3	-4.2	8.8	14.7	36.6	-11.3
26	F	61	17.2	8.4	30.7	-35.0	10	0	8	11.7	1.2	27.8	-29.8	9.0	9.4	27.1	-10.4
27	F	49	10.7	37.0	48.2	-28.7	10	0	10	5.3	34.1	47.7	-27.4	4.0	22.4	38.0	-18.2
28	M	24	14.2	35.2	52.7	-16.9	7	0	7	2.6	32.6	51.4	-7.8	7.6	22.7	41.5	-12.6
29	F	36	9.3	23.7	41.2	-11.2	0	0	7	3.1	-0.5	20.2	-0.1	8.5	18.5	34.8	-9.1
30	F	59	4.5	29.0	45.4	-25.5	9	0	8	-3.6	19.5	39.5	-21.1	-0.3	16.6	35.0	-16.0
31	M	66	2.7	8.8	27.1	-28.7	8	0	11	-1.5	17.2	34.3	-23.5	1.4	7.8	27.7	-13.7
32	F	18	9.9	21.6	40.6	-14.9	0	0	6	4.2	7.8	26.9	-1.6	10.4	18.9	37.2	-13.6
33	M	18	13.5	20.2	35.7	-22.9	9	6	8	6.7	5.5	23.9	-8.7	2.9	6.1	24.2	-8.3
34	M	71	17.8	15.0	33.9	-23.1	11	0	8	3.5	6.9	28.2	-11.7	5.0	7.5	26.5	-5.4

F, female; M, male; age in years. MDCO, medial displacement calcaneal osteotomy; LCL, lateral column lengthening.

radiographic effects remain difficult to quantify. The omission of soft-tissue procedures from the algorithm likely contributed to the observed variability, consistent with Deland et al., who identified the spring and deltoid ligaments as secondary stabilizers of the medial column in PCFD [24]. Variability in tissue quality and tensioning limits incorporation into predictive models and likely contributed to case-level variability. Soft tissue balance remains an important target for future refinement.

Several study limitations warrant consideration. First, the sample size was moderate, and follow-up was limited to three months, restricting assessment of long-term maintenance of correction. However, the primary aim was to compare model-predicted alignment with postoperative correction under full weightbearing; longer-term follow-up would introduce

additional variables such as accommodation and loss of correction [25]. Second, the predictive model was developed using a combination of surgically treated PCFD cases and cadaveric specimens subjected to isolated and/or combined procedures (MDCO, LCL, CO) of varying magnitudes. The use of cadaveric models may introduce bias, as alignment changes following surgical intervention in cadaveric tissue do not fully replicate those in living patients. In addition, combining cadaveric and patient-derived data may influence model generalizability. Nevertheless, cadaveric specimens enabled assessment of isolated and combined procedure effects, which is rarely feasible clinically. Third, the current predictive model accounts only for bony procedures and does not incorporate soft-tissue contributions, which can significantly influence alignment. For example, spring ligament

Table 3
Combined overview of preoperative metrics, postoperative outcomes of the real cases, and the simulated predicted scenario in the current study ($N = 34$).

Metric	Preoperative	Real Postoperative	Δ (Preoperative -Real Postoperative)	Predicted Postoperative	Δ (Preoperative -Predicted Postoperative)
HMA (Class A PCFD)	12.0 (6.12)	2.9 (6.40)	-10.0 (6.92)	5.7 (3.72)	-7.3 (4.56)
TFMA-A (Class B PCFD)	24.1 (7.82)	15.9 (11.45)	-8.2 (10.11)	15.7 (6.52)	-8.4 (4.95)
TNCA (Class B PCFD)	42.4 (6.46)	33.8 (9.91)	-8.6 (9.65)	34.2 (5.41)	-8.2 (4.19)
TFMA-S (Class C PCFD)	-25.3 (8.20)	-14.5 (10.90)	10.8 (7.79)	-12.4 (5.01)	13.0 (7.91)

The differences between pre- and postoperative measurements are expressed as Δ (delta). Hindfoot Moment Arm (HMA) values are reported in millimeters, while all other parameters, including talus–first metatarsal angle axial plane (TFMA-A), talonavicular coverage angle (TNCA), and talus–first metatarsal angle sagittal plane (TFMA-S) are expressed in degrees. Measurements are presented as mean and standard deviation (SD).

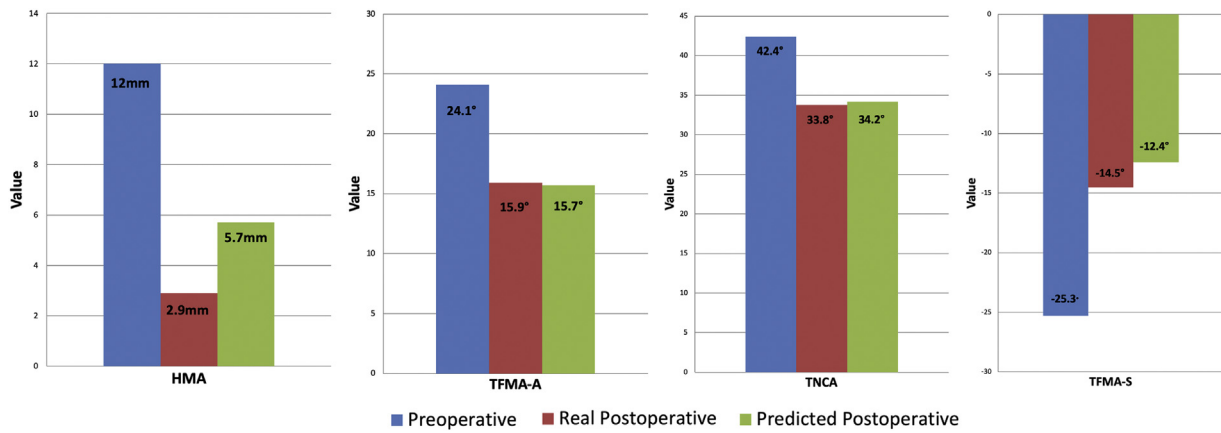


Fig. 2. Bar charts illustrating preoperative, real postoperative, and predicted postoperative alignment values derived from the model for each of the four key deformity parameters: hind-foot moment arm (HMA, mm), talus–first metatarsal angle in the axial plane (TFMA-A, °), talonavicular coverage angle (TNCA, °), and talus–first metatarsal angle in the sagittal plane (TFMA-S, °). Values represent cohort means. Real postoperative measurements reflect the achieved correction, while predicted values represent algorithm-estimated postoperative alignment based on surgeon-selected osteotomy magnitudes.

reconstruction or augmentation may assist in correcting hindfoot valgus and midfoot/forefoot abduction (PCFD Classes A and B), while flexor digitorum longus (FDL) transfer to the navicular and peroneus brevis to longus transfer may help restore midfoot/forefoot abduction and medial arch height (PCFD Classes B and C) [11,26]. Fourth, correction of Class D deformity was not modeled, despite the known role of peritalar subluxation in deformity progression [16]. Incorporating parameters for Class D deformity will be essential in future developments. Finally, this study included only flexible PCFD treated with joint-sparing reconstruction (stage 1), limiting generalizability to rigid deformities requiring arthrodesis (stage 2).

Despite these limitations, this study advances WBCT-based computational planning by testing and validating a WBCT-based predictive surgical planning model against true postoperative 3D alignment. To our knowledge, this represents the first comparison of model-predicted alignment outcomes with postoperative WBCT results in PCFD [11–13,23]. Thus, this work represents an important step toward data-driven, patient-specific WBCT-based surgical planning in PCFD. Predictive planning tools may not only estimate postoperative alignment based on intraoperative procedure magnitudes but also support surgeon decision-making regarding the optimal combination and magnitude of osteotomies tailored to each patient’s unique deformity pattern as visualized on preoperative WBCT.

Future research should focus on expanding the predictive model to incorporate soft-tissue behavior, dynamic loading conditions, and

larger, multi-surgeon datasets to enable more comprehensive and patient-specific modeling. The long-term goal is to develop WBCT-based planning tools capable of recommending individualized correction magnitudes directly from preoperative imaging, rather than relying solely on surgeon experience. Integration with intraoperative navigation or augmented reality could further enable real-time adjustment of osteotomy magnitude based on predicted alignment effects. Finally, correlating WBCT-based alignment changes with patient-reported outcomes will be crucial for determining which radiographic corrections most meaningfully translate into functional improvement and recovery.

Conclusion

This study evaluated the effectiveness of a WBCT-based predictive surgical planning model for patients with flexible PCFD undergoing joint-sparing reconstruction. The model reliably estimated postoperative alignment when actual intraoperative bony correction magnitudes were applied.

The model demonstrated the highest predictive accuracy for hind-foot valgus correction (Class A PCFD), supporting the primary study objective. While mean correction of midfoot/forefoot abduction (Class B) and arch collapse (Class C) was accurately estimated, greater case-level variability was observed, suggesting areas for further refinement. By validating model-predicted alignment against true postoperative WBCT data, this study demonstrates the feasibility of data-driven, patient-specific surgical planning for PCFD. Future work should focus on incorporating soft-tissue effects, multiplanar coupling, and individualized biomechanical modeling. With continued development, such predictive planning tools may support surgeon decision-making regarding optimal corrective procedures and magnitudes tailored to each patient’s unique deformity, thereby improving surgical outcomes and advancing the standard of care for PCFD.

Authors contributions

Wolfram Grün MD: Original idea, Data collection, Manuscript writing, Submission, Pierre-Henri Vermorel, MD: Data collection, Manuscript writing, Antoine Acker MD: Data collection, Manuscript editing, Emily Luo MHS: Data collection, Manuscript editing, Enrico Pozzessere MD: Data collection, Manuscript writing, Scott J. Ellis MD: Manuscript

Table 4

Overview of algorithm performance metrics for all radiographic parameters (Hindfoot Moment Arm-HMA, Talus–First metatarsal angle axial plane-TFMA-A, talonavicular coverage angle-TNCA, and Talus–First metatarsal angle sagittal plane-TFMA-S) in the simulated scenario (N = 34).

Parameter	Mean Bias ± SD	p value	95% LoA (Lower–Upper)	MAE	RMSE
HMA	2.73 ± 5.30	0.005	–7.66 / 13.12	≈ 2.9	≈ 3.7
TFMA-A	–0.20 ± 9.00	0.90	–17.84 / 17.44	≈ 4.2	≈ 6.0
TNCA	0.39 ± 8.43	0.79	–16.13 / 16.91	≈ 4.0	≈ 5.9
TFMA-S	2.13 ± 9.75	0.21	–16.98 / 21.23	≈ 4.5	≈ 6.5

The table summarizes the agreement between algorithm-predicted and true postoperative WBCT measurements. “Mean Bias ± SD” indicates the mean difference between predicted and real postoperative values (Predicted – Real). Positive bias reflects overestimation of correction, whereas negative bias reflects underestimation. The 95% limits of agreement (LoA) were derived from the mean bias ± 1.96 × SD. Paired t-tests assess systematic differences between predicted and actual values. MAE, mean absolute error; RMSE, root-mean-square error; SD, standard deviation.

editing, François Lintz MD, PhD: Manuscript writing, Cesar de Cesar Netto MD, PhD: Original idea, Data collection, Manuscript editing.

Statements and Declarations—Ethical considerations

Our Institutional review board (IRB) approved this study (IRB number Pro00113556).

Consent to participate

Not applicable.

Consent for publication

Not applicable.

Declaration of conflicting interest

Wolfram Grün MD: None.

Pierre-Henri Vermorel, MD: None.

Antoine Acker MD: CurveBeamAI (shareholder).

Emily Luo BS: Sana Biotechnology (shareholder).

Enrico Pozzessere MD: None.

Scott J. Ellis MD: Paragon28 (consultant), CurvebeamAI (consultant).

François Lintz MD, PhD: Paragon28 (consultant, shareholder), CurvebeamAI (consultant, shareholder), Newclip Technics (consultant, royalties), Podonov (consultant, royalties), LINNOV (founder, shareholder), Followinvest (shareholder), International WBCT Society (co-founder, past-president).

Cesar de Cesar Netto MD, PhD: Paragon28 (consultant, medical advisory board, royalties), CurvebeamAI (consultant, shareholder), Ossio (consultant), Zimmer (consultant), Stryker (consultant), International WBCT Society (co-founder, President), exactech (consultant), arthrex (consultant), tayco brace (shareholder), extremity medical (consultant), aofas committee member, foot ankle clinics (editor in chief).

Funding statement

No funding was received for this study.

References

- [1] de Cesar Netto C, Deland JT, Ellis SJ. Guest Editorial: expert consensus on adult-acquired flatfoot deformity. *Foot Ankle Int* 2020;41(10):1269–1271. <https://doi.org/10.1177/1071100720950715>.
- [2] Myerson MS, Thordarson DB, Johnson JE, et al. Classification and nomenclature: progressive collapsing foot deformity. *Foot Ankle Int* 2020;41(10):1271–1276. <https://doi.org/10.1177/1071100720950722>.
- [3] Sangeorzan BJ, Hintermann B, de Cesar Netto C, et al. Progressive collapsing foot deformity: consensus on goals for operative correction. *Foot Ankle Int* 2020;41(10):1299–1302. <https://doi.org/10.1177/1071100720950759>.
- [4] Ellis SJ, Johnson JE, Day J, et al. Titrating the amount of bony correction in progressive collapsing foot deformity. *Foot Ankle Int* 2020;41(10):1292–1295. <https://doi.org/10.1177/1071100720950741>.
- [5] Thordarson DB, Schon LC, de Cesar Netto C, et al. Consensus for the indication of lateral column lengthening in the treatment of progressive collapsing foot deformity. *Foot Ankle Int* 2020;41(10):1286–1288. <https://doi.org/10.1177/1071100720950732>.
- [6] Johnson JE, Sangeorzan BJ, de Cesar Netto C, et al. Consensus on indications for medial cuneiform opening wedge (Cotton) osteotomy in the treatment of progressive collapsing foot deformity. *Foot Ankle Int* 2020;41(10):1289–1291. <https://doi.org/10.1177/1071100720950739>.
- [7] Schon CL, de Cesar Netto C, Day J, et al. Consensus for the indication of a medializing displacement calcaneal osteotomy in the treatment of progressive collapsing foot deformity. *Foot Ankle Int* 2020;41(10):1282–1285. <https://doi.org/10.1177/1071100720950747>.
- [8] Conti MS, Ellis SJ, Chan JY, Do HT, Deland JT. Optimal position of the heel following reconstruction of the stage II adult-acquired flatfoot deformity. *Foot Ankle Int* 2015;36(8):919–927. <https://doi.org/10.1177/1071100715576918>.
- [9] Conti MS, Chan JY, Do HT, Ellis SJ, Deland JT. Correlation of postoperative midfoot position with outcome following reconstruction of the stage II adult acquired flatfoot deformity. *Foot Ankle Int* 2015;36(3):239–247. <https://doi.org/10.1177/1071100714564217>.
- [10] Conti MS, Garfinkel JH, Kunas GC, Deland JT, Ellis SJ. Postoperative medial cuneiform position correlation with patient-reported outcomes following cotton osteotomy for reconstruction of the stage II adult-acquired flatfoot deformity. *Foot Ankle Int* 2019;40(5):491–498. <https://doi.org/10.1177/1071100718822839>.
- [11] Chan JY, Williams BR, Nair P, et al. The contribution of medializing calcaneal osteotomy on hindfoot alignment in the reconstruction of the stage II adult acquired flatfoot deformity. *Foot Ankle Int* 2013;34(2):159–166. <https://doi.org/10.1177/1071100712460225>.
- [12] Chan JY, Greenfield ST, Soukup DS, Do HT, Deland JT, Ellis SJ. Contribution of lateral column lengthening to correction of forefoot abduction in stage IIb adult acquired flatfoot deformity reconstruction. *Foot Ankle Int* 2015;36(12):1400–1411. <https://doi.org/10.1177/1071100715596607>.
- [13] Kunas GC, Do HT, Aiyyer A, Deland JT, Ellis SJ. Contribution of medial cuneiform osteotomy to correction of longitudinal arch collapse in stage IIb adult-acquired flatfoot deformity. *Foot Ankle Int* 2018;39(8):885–893. <https://doi.org/10.1177/1071100718768020>.
- [14] De Cesar Netto C, Godoy-Santos AL, Saito GH, et al. Subluxation of the middle facet of the subtalar joint as a marker of peritalar Subluxation in adult acquired flatfoot deformity: a case-control study. *J Bone Jt Surg - Am* 2019;101(20):1838–1844. <https://doi.org/10.2106/JBJS.19.00073>.
- [15] Dibbern KN, Li S, Vivtcharenko V, et al. Three-dimensional distance and coverage maps in the assessment of peritalar subluxation in progressive collapsing foot deformity. *Foot Ankle Int* 2021;42(6):757–767. <https://doi.org/10.1177/1071100720983227>.
- [16] de Cesar Netto C, Barbachan Mansur NS, Talaski G, et al. From asymptomatic flatfoot to progressive collapsing foot deformity. *J Bone Jt Surg* 2025;107(18):2060–2068. <https://doi.org/10.2106/JBJS.24.01619>.
- [17] de Cesar Netto C, Barbachan Mansur NS, Lalevee M, et al. Effect of peritalar subluxation correction for progressive collapsing foot deformity on patient-reported outcomes. *Foot Ankle Int* 2023;44(11):1128–1141. <https://doi.org/10.1177/10711007231192479>.
- [18] Mansur NSB, Lalevee M, Shamrock A, Lintz F, De Carvalho KAM, De Cesar Netto C. Decreased peritalar subluxation in progressive collapsing foot deformity with ankle valgus tilting. *JBJS Open Access* 2023;8:4. <https://doi.org/10.2106/JBJS.OA.23.00025>.
- [19] De Cesar Netto C, Ahrenholz S, lehl C, et al. Lapidcotton technique in the treatment of progressive collapsing foot deformity. *J Foot Ankle* 2020;14(3):301–308. <https://doi.org/10.30795/jfootankle.2020.v14.1215>.
- [20] Mansur NSB, Fayed A, Chinelati R, Schmidt E, Lalevee M, de Cesar Netto C. Allograft bone-block plantarflexion first tarsometatarsal arthrodesis: short-term outcomes. *Foot Ankle Int* 2025;46:1248–1258. <https://doi.org/10.1177/10711007251363926>. Published online.
- [21] Bland JM, Altman DG. Statistical methods for assessing agreement between two methods of clinical measurement. *Lancet* 1986;327(8476):307–310 <http://www.ncbi.nlm.nih.gov/pubmed/2868172>.
- [22] Sangeorzan BJ, Mosca V, Hansen ST. Effect of calcaneal lengthening on relationships among the Hindfoot, Midfoot, and Forefoot. *Foot Ankle* 1993;14(3):136–141. <https://doi.org/10.1177/107110079301400305>.
- [23] Smith BA, Adelaar RS, Wayne JS. Patient specific computational models to optimize surgical correction for flatfoot deformity. *J Orthop Res* 2017;35(7):1523–1531. <https://doi.org/10.1002/jor.23399>.
- [24] Deland JT, de Asla RJ, Sung IH, Ernberg LA, Potter HG. Posterior tibial tendon insufficiency: which ligaments are involved? *Foot Ankle Int* 2005;26(6):427–435. <https://doi.org/10.1177/107110070502600601>.
- [25] Abousayed MM, Coleman MM, Wei L, de Cesar Netto C, Schon LC, Guyton GP. Radiographic outcomes of cotton osteotomy in treatment of adult-acquired flatfoot deformity. *Foot Ankle Int* 2021;42(11):1384–1390. <https://doi.org/10.1177/10711007211015175>.
- [26] Conti MS, Kim J, Hoffman J, et al. Peroneus Brevis to Longus Tendon transfer in the treatment of flexible progressive collapsing foot deformity: a cadaveric study. *Foot Ankle Int* 2024;45(6):656–663. <https://doi.org/10.1177/10711007241238209>.